

Supporting information

Flexible Sb₂O₃/carbon cloth composite as a free-standing high performance anode for sodium ion batteries

Jie Fei, Yali Cui, Jiayin Li, Zhanwei Xu, Jun Yang, Ruiyi Wang, Yayi Cheng,

Jianfeng Huang*

College of Material Science & Engineering, Shaanxi University of Science and Technology, Shaanxi 710021, P. R. China

E-mail: Huang Jianfeng@sust.edu.cn

1. Experimental Section

Preparation of carbon cloth substrate. Using carbon cloth (CC) supplied by Weihai Guangwei Group Co. Ltd., China as templates, flexible Sb₂O₃/CC anodes were fabricated by a simple solvothermal method. Before the fabrication of Sb₂O₃ samples, the CC was cleaned by sonication sequentially in acetone, deionized water, and ethanol for 30 min each and then anodized in electrodeposition equipment at 5V for 2 minutes. After dried, the CC substrate was obtained.

Synthesis of Sb₂O₃/CC and pure Sb₂O₃ samples. Flexible Sb₂O₃/CC composite was synthesized via a two-step process. In a typical process, 2.5 mmol of SbCl₃ was first dissolved in 40mL anhydrous ethanol to form homogeneous solution. NaOH solution was added to homogeneous solution until formed a sol solution under vigorous stirring. After dipping CC (5 cm×5 cm) in sol solution and drying for 3 times, keep adding NaOH solution until the pH of solution reached 8-9. The solution and CC was then transferred into a Teflon-lined stainless autoclave. The autoclave was sealed and maintained at 150 °C for 6 h. After the autoclave cooled down to room temperature, the product was collected, washed, vacuum dried. Pure Sb₂O₃ was also prepared under the same condition without CC.

Electrochemical Measurement of Sodium-ion Batteries.

CC with Sb₂O₃ nanospheres covered was first cut into many smaller round pieces with the diameter of 16 mm. Both Sb₂O₃/CC and CC electrodes were weighed in a high-precision analytical balance (Sartorius, max weight 5100 mg, *d*=0.001 mg). The

reading difference was the exact mass for the coated Sb_2O_3 on CC. The loading density of the Sb_2O_3 active materials is calculated as $0.1\sim 0.2\text{ mg/cm}^2$. The electrochemical performance of the Sb_2O_3 was investigated by using it as anode in coin-type half-cells, which were laboratory-assembled by a CR2032 press in an argon-filled glove box. A Cu foil was used as the counter electrode and reference electrodes. Flexible $\text{Sb}_2\text{O}_3/\text{CC}$ composite was used directly as the working electrode without any polymeric binder or carbon black conductive additives. The electrolyte was a mixture of ethylene carbonate and dimethyl carbonate 1:1 (w/w) containing 1 M NaClO_4 and 5 wt% fluoroethylene carbonate additive. The galvanostic charge/discharge tests were conducted using a New are battery testing system under different current density with a voltage range of 0.01-3.0 V (vs Na/Na^+). Cyclic voltammetry and electrochemical impedance spectroscopy were conducted using a CHI 600D electrochemistry workstation.

Characterizations: X-ray diffraction (XRD) patterns were obtained using a Rigaku (Japan, D/max-2200PC) with Cu $K\alpha$ radiation ($\lambda=1.5406\text{ \AA}$) in the 2θ ranging from 15 to 70. X-ray photoelectron spectra (XPS) were conducted using a Surface Science Instruments Spectrometer focused on monochromatic Al $K\alpha$ radiation (1486.6 eV). The morphology and microstructure of the samples were observed using field emission scanning electron microscope (FESEM, Hitachi, S-4800) and transmission electron microscope (TEM, TecnaiG2F20S-TWIN).

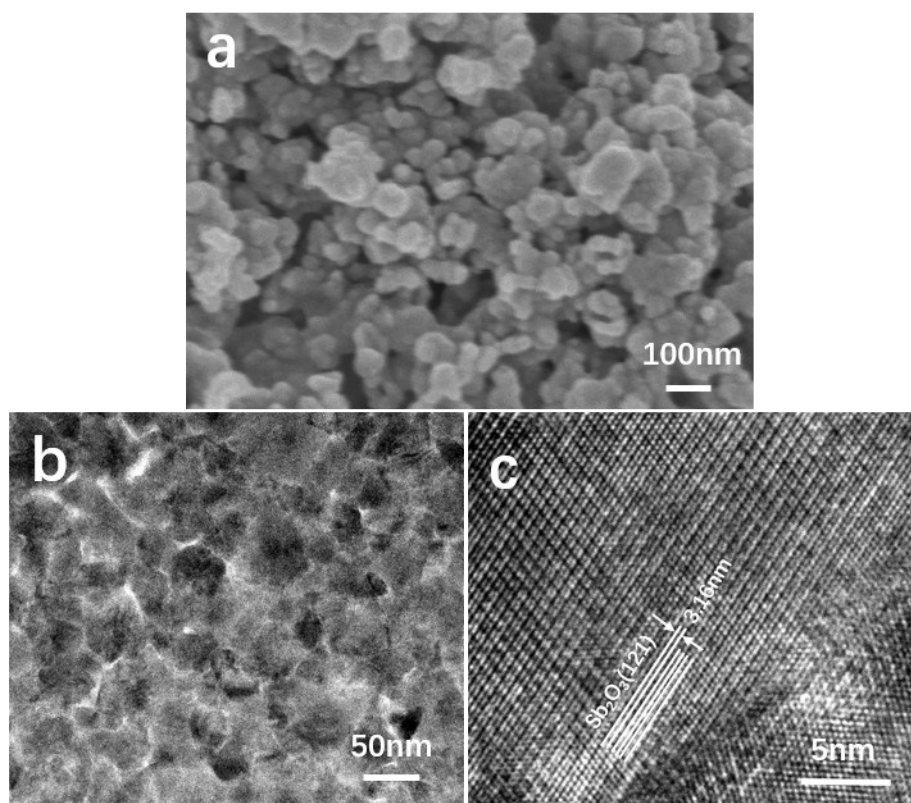


Figure. S1 (a) FESEM, (b) TEM and (c) HRTEM micrographs of pure Sb_2O_3 .

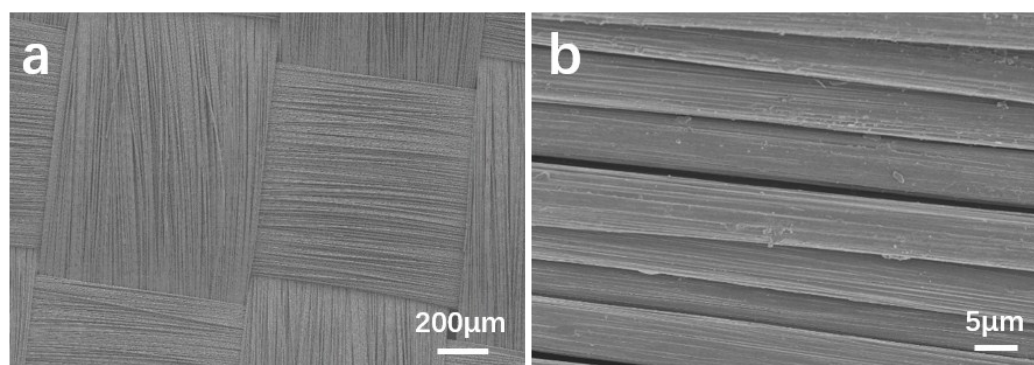


Fig. S2 (a) Low and (b) high resolution SEM micrographs of CC.

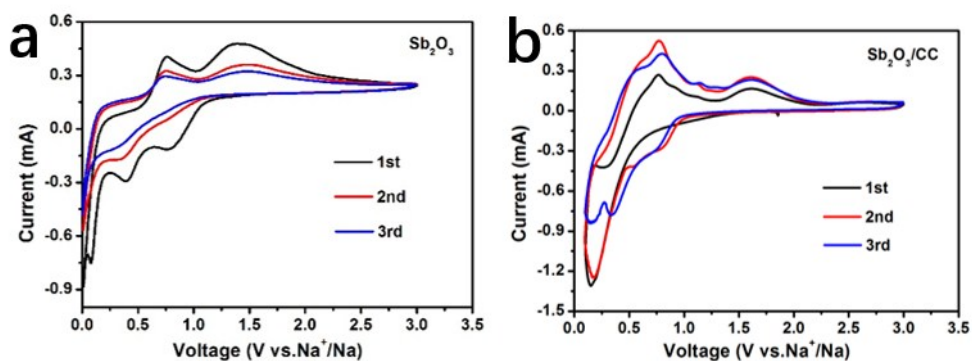


Fig. S3 CV curves of the (a) Sb_2O_3 and (b) $\text{Sb}_2\text{O}_3/\text{CC}$ electrode at first third cycles.

Fig. S3 display the CV curves of pure Sb_2O_3 and $\text{Sb}_2\text{O}_3/\text{CC}$ electrode which were measured at a scan rate of 0.1 mV/s between 0 and 3V (vs Na/Na^+). For pure Sb_2O_3 electrode, it can be observed that the first cathodic scan is different from the following cathodic scans. During the first reduction scan, a reduction peak at 0.75 V in the first cycle assigned to the conversion reaction between Sb_2O_3 and Na^+ (reaction 1) almost disappears in the 2nd and 3rd cycles, suggesting that the first step reveals weak reversibility. Moreover, a cathodic peak at 0.4 V is observed corresponding to the formation of the solid electrolyte interface (SEI) and the alloying reaction between Sb and Na^+ . In the following cycles, the cathodic peaks gradually stabilize at 0.35 V, demonstrating that the alloying reaction is reversible. During the reverse anodic scans, two oxidative peaks positioned at around 0.75 and 1.35 V are assigned to the dealloying reaction of Na-Sb compounds and the extraction of Na^+ from Na_2O . As for $\text{Sb}_2\text{O}_3/\text{CC}$, the CV curves are similar to those of Sb_2O_3 . However, there still exists some differences. During the anodic scans, the reduction peak at 0.75 V assigned to the conversion reaction between Sb_2O_3 and Na^+ (reaction 1) still appears in 3rd cycle and the oxidative peak at 0.75 V assigned to the dealloying reaction of Na-Sb compounds is stronger than Sb_2O_3 electrode, suggesting that the $\text{Sb}_2\text{O}_3/\text{CC}$ electrode shows higher reversibility. These differences should be ascribed to the uniform Sb_2O_3 on highly conductive CC and strong chemical bonds between Sb_2O_3 and CC. In addition, there appears a flat peak at 2.5-3.0V, for the reason that the incorporation of

CC into Sb_2O_3 leads to lower polarization and then causes the conversion reaction of Sb_2O_3 to Sb_2O_5 , which is in good agreement with the following XPS results

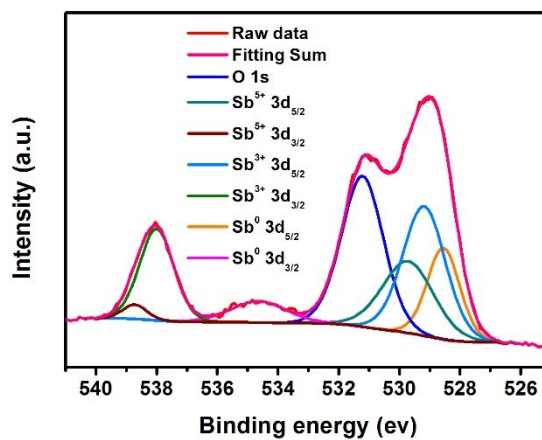


Fig. S4 XPS spectra of the $\text{Sb}_2\text{O}_3/\text{CC}$ composite at 2.7V charged state at a current density of 0.05 A g^{-1} after 100 cycles: Sb3d and O1s.

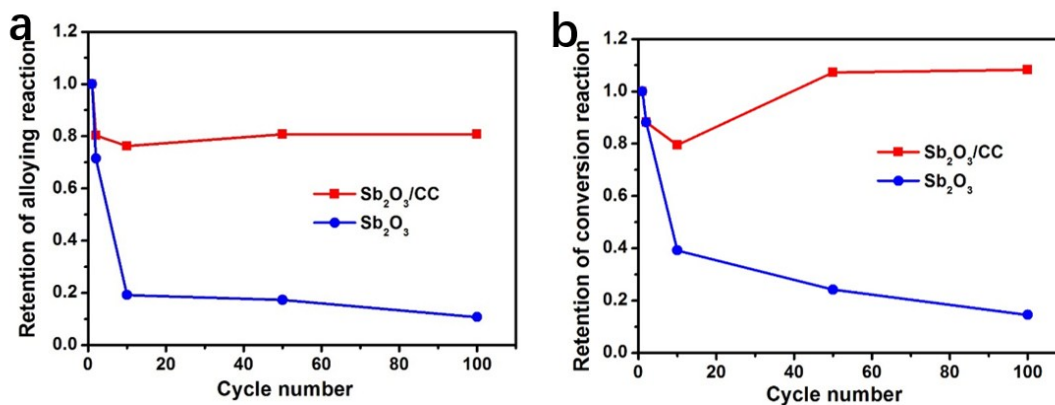


Fig. S5 (a, b) The charge capacity retention of the alloying and conversion reaction at the 1st, 2nd, 10th, 50th and 100th cycles.

Table 1 Cycling performance comparison of the as-prepared $\text{Sb}_2\text{O}_3/\text{CC}$ composite with previously reported Sb-based anodes

| Materials | Current density /A g ⁻¹ | First cycle capacity /mA h g ⁻¹ | Cycles | Final cycle capacity /mA h g ⁻¹ |
|---|------------------------------------|--|--------|--|
| Sb/C^{10} | 0.05 | 554 | 200 | 315(0.5A g ⁻¹) |
| Sb/C^{11} | 0.1 | 948 | 240 | 407 |
| ZnSb^{12} | 0.02 | 438(second) | 100 | 377 |
| $\text{Sb}_2\text{S}_3/\text{graphene}^{13}$ | 0.05 | 710 | 100 | 589.3 |
| $\text{Sb}_2\text{S}_3/\text{SGS}^{14}$ | 0.05 | 786.2 | 900 | 524(2A g ⁻¹) |
| $\text{Sb}_2\text{O}_4^{15}$ | 0.1 | 1083.8 | 50 | 700 |
| $\text{Sb}_2\text{O}_4/\text{RGO}^{16}$ | 0.1 | 944 | 100 | 890 |
| Sb_2O_3 film ¹⁷ | 0.5 | 645 | 200 | 414 |
| $\text{Sb}_2\text{O}_3/\text{RGO}^{18}$ | 0.1 | 854.6 | 50 | 503 |
| $\text{Sb}_8\text{O}_{11}\text{Cl}_2^{19}$ | 0.05 | 774.3 | 40 | 362.9 |
| $\text{Sb}_2\text{O}_3/\text{CC}$ (this work) | 0.05 | 1248 | 100 | 900 |

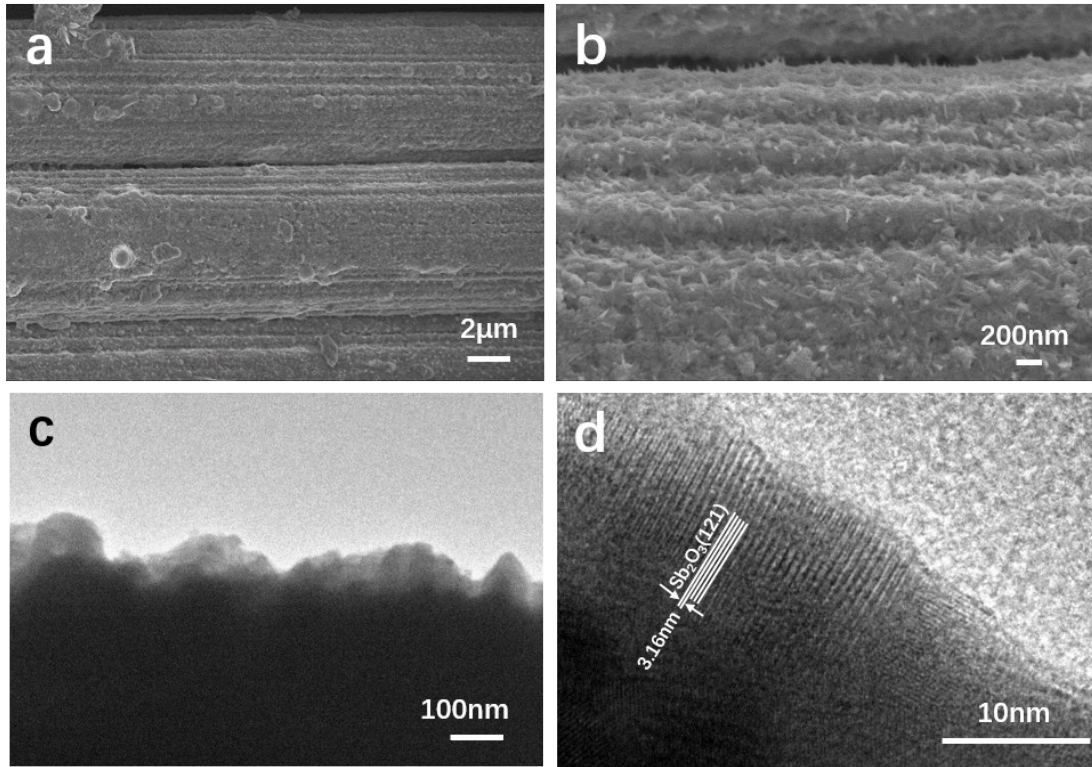


Figure. S6 (a, b) SEM, TEM (b) and HRTEM (c) micrographs of $\text{Sb}_2\text{O}_3/\text{CC}$ composite after 100 cycles.

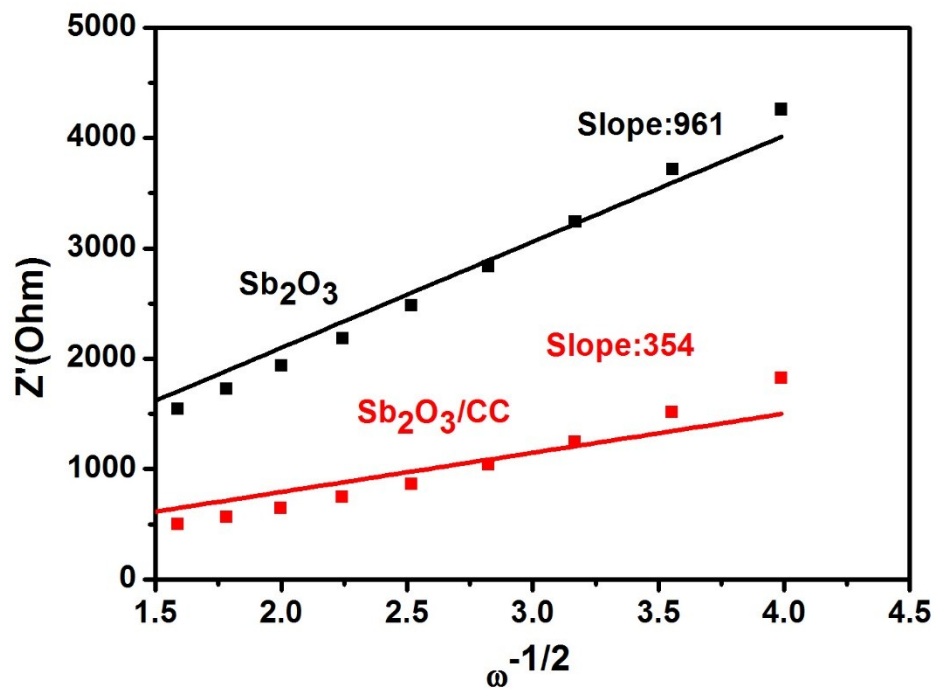


Figure. S7 Dependence of Z_{re} on the reciprocal square root of the frequency in the low-frequency region of the $\text{Sb}_2\text{O}_3/\text{CC}$ composite.

The symbols: R_e , R_f , R_{ct} , ZW and CPE stand for the resistance of the electrolyte, resistance of SEI layer, charge transfer resistance, Warburg impedance and constant phase element, respectively. Further, the straight line in the low frequency region is the Warburg behaviour which was attributed to the diffusion of Na^+ in the electrode. We can evaluate the apparent Na^+ diffusion coefficient (D) of the Sb_2O_3 and Sb_2O_3/CC electrode by the following equation 4 and 5:

$$D = (R^2 T^2) / (2 A^2 n^4 F^4 C^2 \sigma^2) \quad (4)$$

$$Z_{re} = R_e + R_{ct} + \sigma \omega^{-1/2} \quad (5)$$

The linear fitting according to equation 5 for the low frequency region of the EIS plots shows in Figure S7.